

Rb-Sr and $^{40}\text{Ar}/^{39}\text{Ar}$ Mineral Ages of Granitoid Intrusives in the Mabujina Unit, Central Cuba: Thermal Exhumation History of the Escambray Massif

*F. Grafe,^{1,2} K. P. Stanek, A. Baumann,¹ W. V. Maresch,²
W. E. Hames,³ C. Grevel, and G. Millan⁴*

*Institut für Geologie, TU Bergakademie Freiberg, Bernhard von Cotta-Strasse 2, 09596 Freiberg, Germany
(e-mail: grafe@web.de)*

ABSTRACT

We present new and critical isotopic data for late- to postkinematic granitoid intrusions and their epidote-amphibolite-facies country rocks (Mabujina unit) in central Cuba. The Mabujina unit tectonically overlies a nappe sequence of high-pressure (HP) metamorphic rocks in the Escambray Massif. These granitoid rocks have a variable granodioritic to granitic composition, are generally rich in large ion lithophile elements, and resemble normal midocean ridge basalts in their high field strength element concentrations. On the basis of low initial $^{87}\text{Sr}/^{86}\text{Sr}$ ratios, it is inferred that Sr is very likely to be mantle derived. Primary coarse-grained muscovite from pegmatitic intrusions yields Rb-Sr crystallization ages of ~86–88 Ma (Rio Jicaya region) and ~80–82 Ma (Yayabo region). Laser $^{40}\text{Ar}/^{39}\text{Ar}$ ages for coarse- and fine-grained white mica (72–74 Ma) and Rb-Sr ages for biotite (73 Ma) outline the cooling history of these granitoids and their country rock. Dating of pegmatites within the Mabujina unit places minimum age limits on the epidote-amphibolite-facies metamorphism, on the end of the magmatic activity and initial collision of the Cretaceous island arc, and on the HP metamorphism and juxtaposition of tectonometamorphic units in the Escambray Massif. The combination of the new thermochronological data with constraints from the geological record indicates thermal relaxation during the initial stages of the arc-continent collision.

Introduction

A suture zone between the North American plate and a Cretaceous Caribbean island arc that once was ca. 1500 km long and extended through Hispaniola to Puerto Rico is exposed in central Cuba. In Cuba, the collision between the North American plate and the island arc belonging to the Pacific (Farallon) plate occurred between the Late Cretaceous and the Eocene (Pindell 1993, 1994; Stanek and Voigt 1994; Hutson et al. 1998; Stanek 2000). The Cretaceous island arc initially collided with the offshore sedimentary fan belonging to the Yu-

catán Peninsula (Stanek and Voigt 1994; Stanek 2000) and was subsequently sutured to the North American plate during its collision with the Bahamas Platform (Iturralde-Vinent 1994). However, final overthrusting of the island arc and associated ophiolites onto the passive continental margin of North America is related to the formation of a younger, Paleocene island arc to the south that separated the Cretaceous arc from the Pacific plate. Paleocene to recent postcollisional uplift and associated tectonic as well as climate-driven erosion resulted in exhumation of metamorphic complexes in Cuba now exposed on Isla de Juventud (Isle of Pines), in the Escambray region and in eastern Cuba (fig. 1, inset). The collisional suture in central Cuba remained largely intact and has not been obscured by subsequent large-scale E-W shearing common to most of the Northern and Southern Caribbean plate boundary. Only a few ENE-trending strike-slip faults dismembered this collision zone.

The Escambray region exposes ~1800 km² of

Manuscript received March 28, 2000; accepted March 8, 2001.

¹ Institut für Mineralogie, Zentrallaboratorium für Geochronologie, Westfälische Wilhelms-Universität-Münster, Corrensstr. 24, 48149 Münster, Germany.

² Institut für Geologie, Mineralogie und Geophysik, Ruhr-Universität Bochum, 44780 Bochum, Germany.

³ Department of Geology and Geography, Auburn University, Auburn, Alabama 36830, U.S.A.

⁴ Instituto de Geología y Paleontología, Academia de Ciencias de Cuba, Havana, Cuba.

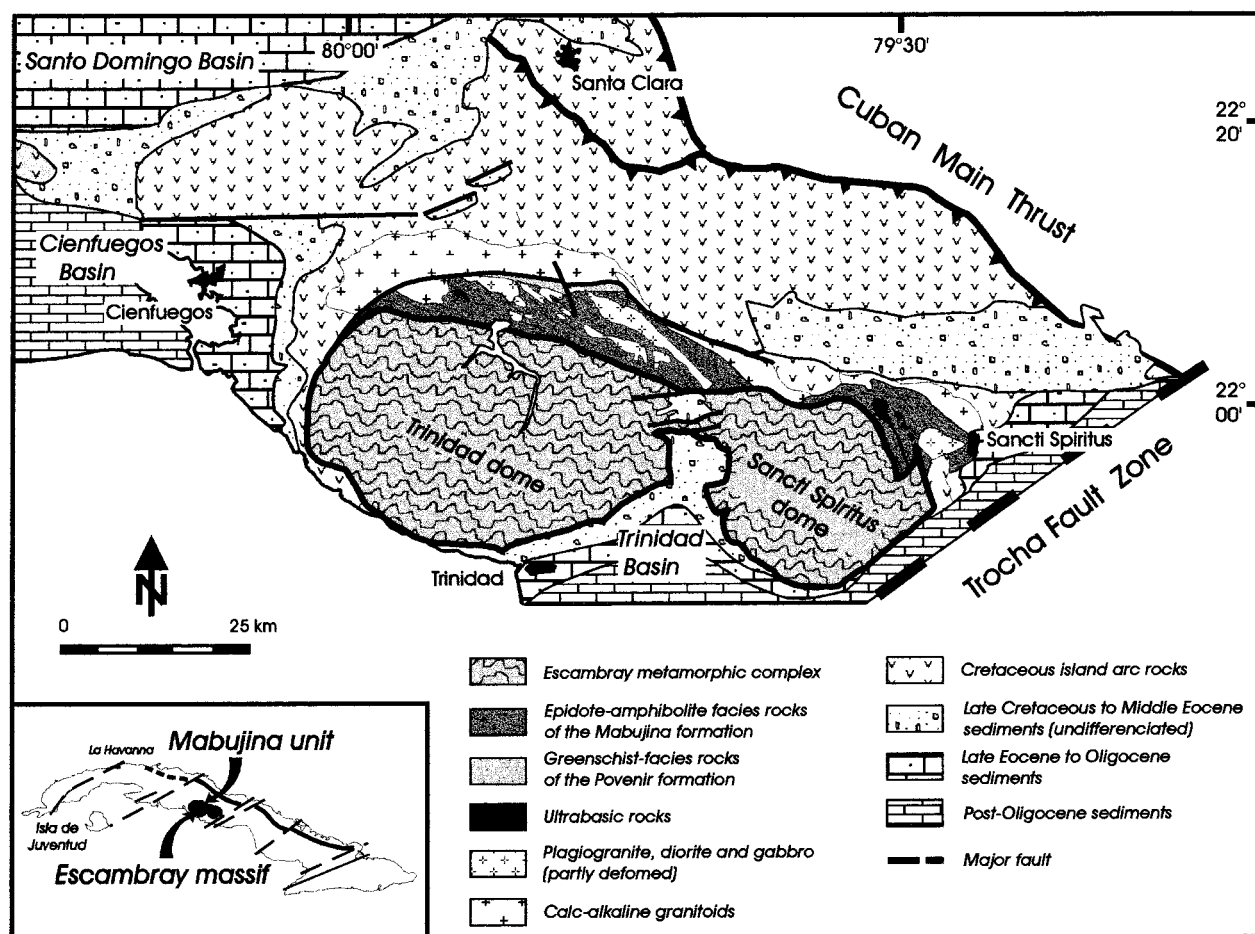


Figure 1. Geological sketch map of central Cuba (Las Villas) modified from Stanek (2000)

crystalline rocks south of the Cuban Main Thrust in a "back-arc" position with respect to the Cretaceous island arc (fig. 1). Most of the metamorphic complex is composed of high-pressure (HP) metamorphic rocks, but marginally the HP rocks are now in tectonic contact with low-pressure amphibolites, which are intruded by granitoid rocks of island arc origin. The age of metamorphism in the Escambray Massif and on the Isla de Juventud is constrained by later Jurassic to Early Cretaceous fauna preserved in metacarbonates (Millan and Myscinski 1978; Somin and Millan 1981). The appearance of pebbles of metamorphic rocks in molassoid sequences in the Middle Eocene indicates the end of the arc-continent collision and final emplacement of the metamorphic units. However, little was previously known about the tectonometamorphic development of this crystalline complex and the metamorphosed parts of the island arc. Existing tectonic models for the Caribbean region

concentrate on the early to mid-Cenozoic history of Cuba (e.g., Pindell 1993, 1994; Iturralde-Vinent 1994). With respect to Cuba, the tectonic development still needs to be clarified, especially in the Late Cretaceous.

In this article we present Rb-Sr and laser-ablation $^{40}\text{Ar}/^{39}\text{Ar}$ age data on late- to postmetamorphic granodiorites and pegmatites, as well as on one sample of their metamorphic country rocks. These data provide critical new constraints on the age of metamorphism and on the uplift, cooling, and exhumation of the Cretaceous island arc in central Cuba.

Geological Setting

Regional Introduction. The Escambray Massif (fig. 1) is a mountainous area consisting of two domelike structures rising more than 1000 m above the flat plains of central Cuba. The western and

eastern parts are called Trinidad dome and Sancti Spiritus dome, respectively. The southern margin is extremely steep. More than 2500 m of relief separate the highest peak from the neighboring sea floor over a horizontal distance of less than 20 km.

Intensive fieldwork since 1994, in conjunction with petrological laboratory study, has led to new geological interpretations for the Escambray Massif. Previous work (e.g., Somin and Millan 1974, 1981; Millan and Somin 1985) suggested a stratigraphic sequence of impure metacarbonates, carbonaceous quartz-mica schists, and metaquartzites. Metabasic bodies of various dimensions are found locally in the form of slightly overprinted gabbro, greenschist, blueschist, eclogite, and amphibolite. Serpentinized ultramafic rocks also occur. On the basis of detailed structural studies in the Sancti Spiritus dome, we now recognize a system of generally flat-lying nappes (Millan 1997; Stanek et al. 1998; Stanek 2000) in the core of this structure, and thus we consider the Escambray metamorphic complex to represent a pile of multiple nappes. In detail, however, different structural interpretations have evolved (Millan 1997; Stanek et al. 1998) and will be discussed in forthcoming articles.

The metamorphic overprint of the carbonate-mica and quartz-mica schists as well as greenschists did not exceed temperatures of $\sim 500^{\circ}\text{C}$. No direct evidence for pressures exceeding 7–8 kbar has so far been found in these rocks (Grevel 2000). Maximum metamorphic conditions of 16–25 kbar, with temperatures ranging from 530° to 610°C , have been determined for blueschists, and 580° to 630°C for eclogites (Grevel 2000). In addition, the occurrence of deerite (Grevel et al. 1996) in interlayered ferruginous metaquartzites of the meta-sedimentary sequence strongly supports the assumption that the whole unit has in fact been affected by HP metamorphism. The uppermost part of the Escambray nappe stack, barroisite-bearing garnet amphibolites of the Yayabo unit (13–14.5 kbar at 580° – 675°C , according to Grevel 2000) have been juxtaposed with epidote-amphibolite-facies rocks of the Mabujina unit.

The Mabujina unit (fig. 2) surrounds the nappes of the Escambray Massif to the north and east in a 5–10-km-wide strip. These predominantly intermediate to mafic metamorphic rocks are referred to in Cuban literature as the Mabujina unit or Mabujina Amphibolites. Such rocks at one time formed the tectonic cover of the Escambray Massif (Somin and Millan 1981; L. Dublan and H. Alvarez, unpub. data, 1986) and were interpreted to represent a deep erosional level within the Cretaceous

island arc forming the backbone of Cuba (Millan and Somin 1985; E. Stanik, J. Manour, and R. Ching, unpub. data, 1981; L. Dublan and H. Alvarez, unpub. data, 1986).

On the basis of metamorphic grade, L. Dublan and H. Alvarez (unpub. data, 1986) distinguished two “formations” in the Mabujina unit. The rocks of the Mabujina “formation” have been folded and metamorphosed to the epidote-amphibolite facies. They are represented mainly by banded porphyroblastic amphibolites, metagabbros, and metadiorites. In some localities near the tectonic contact with the Escambray, higher-grade rocks of the amphibolite facies have also been observed (Millan 1996). However, more acid rocks such as metaplagiogranites and metatonalites also occur. Serpentinized ultrabasic rocks are exposed between steeply dipping fault zones. Locally, late- to post-orogenic granodiorites and associated pegmatites crosscut these metamorphosed island-arc rocks. The greenschist facies Porvenir “formation” is predominated by metamorphosed basaltic volcanics and pyroclastics and has been observed only in boreholes along the northern edge of the Mabujina unit.

We have been able to study in detail the transition between metabasites of the Yayabo nappe and metagabbros/metadiorites of the Mabujina unit in a profile along the Yayabo River near the Yayabo quarry (fig. 2), allowing the contact relationships between the island-arc rocks of the Mabujina unit and the HP nappes to be clarified. The Yayabo and Mabujina units have been juxtaposed along a ductile shear zone about 300 m wide, in which both units have been strongly mylonitized, and a convergence of the mineral assemblages (i.e., metamorphic grade) in both units can be observed. Na-rich amphiboles of the Yayabo unit (barroisite or Na-rich magnesiohornblende and pargasite) reflect a medium- to HP metamorphic regime, whereas the amphiboles in the Mabujina formation (tschermakite and ferropargasite, according to the classification of Leake 1997) suggest a low-pressure regime, although absolute temperatures cannot have differed significantly (e.g., Brown 1977; Laird and Albee 1981a, 1981b). Within the ductile shear zone between the two units, recrystallized amphiboles and core-rim compositional trends thus indicate a convergence mainly of pressures (i.e., depth) at metamorphic conditions intermediate between the dominant overprint of the high- to medium-pressure Yayabo unit and the low-pressure Mabujina formation. Deformation in the amphibolites of both the Yayabo and the Mabujina units was succeeded by static tempering, as indicated by partial

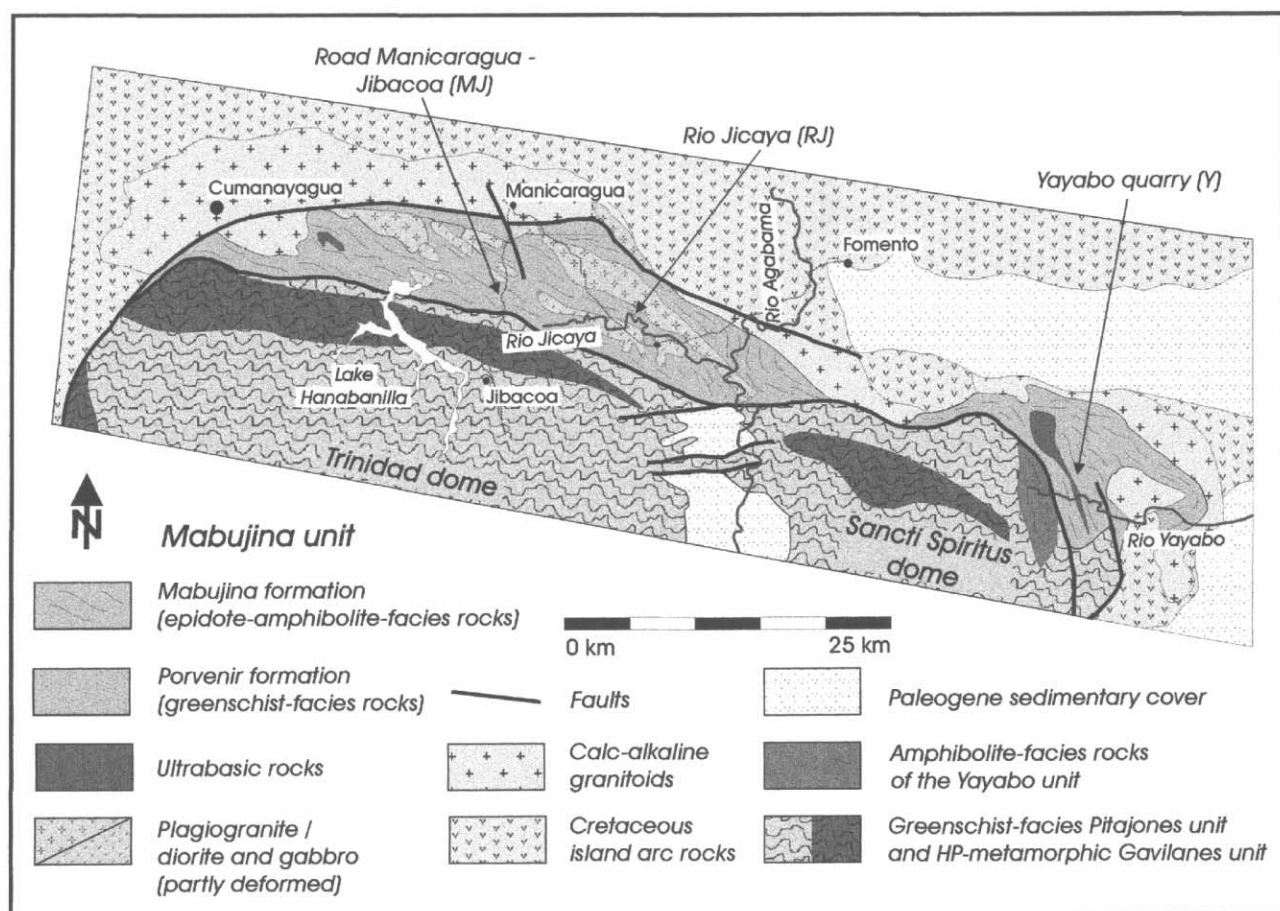


Figure 2. Geological sketch map of the Mabujina unit (Las Villas)

intracrystalline strain recovery and growth of amphibole and plagioclase grains across the mylonitic foliation, indicating that juxtaposition of the two units occurred at depth. It is inferred that the epidote-amphibolite-facies rocks of the Mabujina unit were metamorphosed at <5–9 kbar and temperatures of 610°–730°C before coming into contact with the Yayabo unit.

We have focused on the late- to postorogenic granitoid intrusions in the Mabujina unit because dating of these rocks provides a minimum age for metamorphism and main deformation in the Mabujina unit, as well as for the timing of juxtaposition with the Yayabo unit.

Investigated Samples from the Mabujina Unit. Late- to postorogenic granodiorite and pegmatite, as well as country-rock biotite gneiss, were sampled from different localities in the valley of Rio Jicaya (RJ; figs. 2, 3). Two pegmatite samples were taken from the Yayabo quarry (Y) ~60–80 km to the east (fig. 2). In addition, sill-like pegmatite intru-

sions were sampled along the road from Manicaragua to Jibacoa (MJ), near the tectonic contact between the Mabujina unit and the HP rocks of the Escambray Massif (fig. 2).

The pegmatite samples generally appear unfoliated. Only at locality RJ can a widely spaced sinistral crenulation cleavage be observed. However, kinking of the large crystals of magmatic white mica (fig. 4A) and discrete small shear zones with a new generation of oriented white mica and recrystallized feldspar (fig. 4B) may be observed under the microscope.

Sample F009[RJ] (fig. 3) is actually a pegmatoid apophysis-like vein within a granodiorite F011[RJ]; however, for simplicity of nomenclature, we will also refer to this sample as a pegmatite. Pegmatites are composed of plagioclase, K-feldspar, quartz, white mica, \pm biotite, \pm garnet, secondary epidote (clinozoisite), and chlorite, as well as accessory phases such as zircon and apatite. Laumontite has

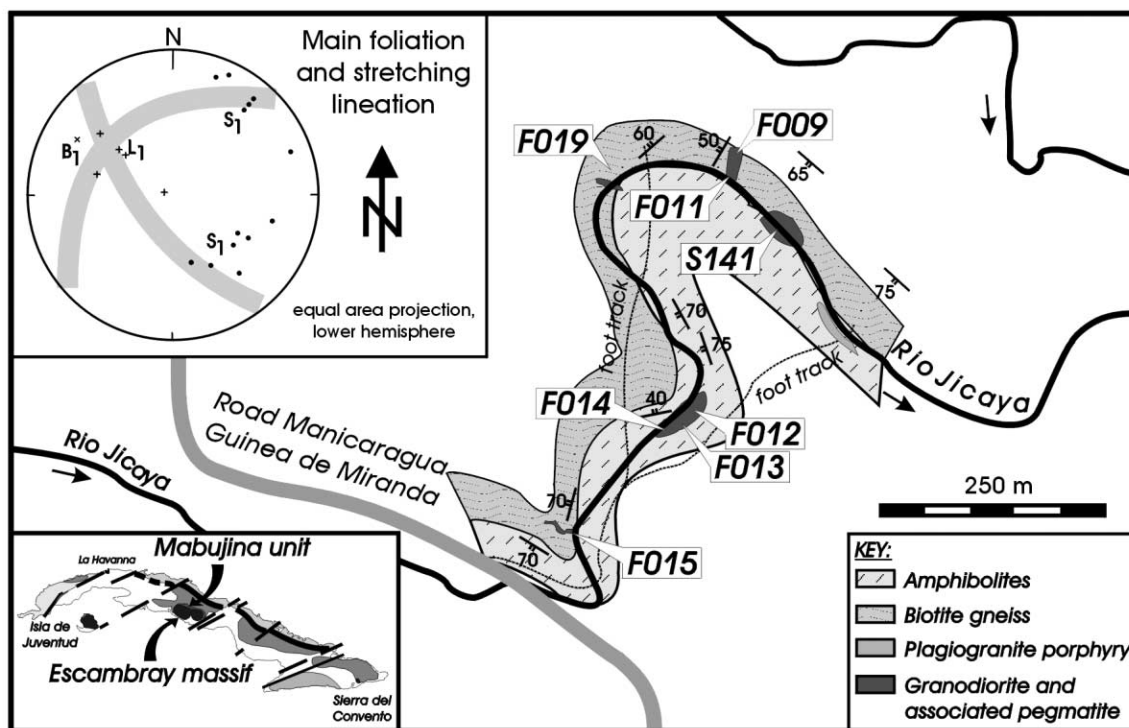


Figure 3. Geological sketch map of the Rio Jicaya valley indicating sample localities

been observed as a secondary product within the splayed edges of kinked primary white mica. Biotite was not found in F009[RJ] and G2057/G2061[Y]. Somin et al. (1992) calculated an age of 85 ± 4 Ma from K-Ar analyses of white mica separated from a pegmatoid quartz-mica vein northwest of the Yayabo quarry, whereas Hatten et al. (1988) determined a K-Ar age of 84 ± 2 Ma on white mica of a pegmatite from Rio Jicaya.

The granodiorites have a mineral content similar to that of the pegmatites, but a smaller grain size. At the well-exposed locality RJ, macro-scale folding can be mapped in the surrounding country rock (fig. 3, inset) with the granitoid intrusions occupying the crests of these folds. The late- to postorogenic granodiorites are massive or only slightly foliated magmatic bodies. Notably, at sample locality F011[RJ], the intrusive contact of the granodiorite to the biotite-gneiss country rock is overprinted by the same deformation, leading to the shearing within the granitoid bodies themselves. Sukar and Perez (1997) reported U-Pb data on zircon of ~ 92 Ma analyzed by Hatten (C. Hatten, pers. comm. to K. Sukar and M. Perez), which can be interpreted as an intrusion age for the granodiorites.

The biotite gneiss is a medium- to fine-grained, well-foliated rock. It is composed of quartz, feld-

spar, biotite, and green amphibole, locally accompanied by garnet, chlorite, white mica, epidote, apatite, and zircon. Bibikova et al. (1988) classified this rock as volcanogenic, on the basis of the morphology of zircons. Bibikova et al. (1988) also reported uranium-lead zircon ages of 110 ± 15 Ma for this rock type, but the geological meaning of this age is unclear since it is based on the apparent $^{206}\text{Pb}/^{238}\text{U}$ age of only one analysis of discordant zircons. Somin and Millan (1981) analyzed whole-rock samples of Mabujina Amphibolite from the region S and SE of Manicaragua (near locality MJ in fig. 2). Using the conventional K-Ar method, they obtained ages ranging from 81 ± 2 to 89 ± 3 Ma. Hatten et al. (1988) determined K-Ar ages of 95 ± 2 and 70 ± 1 Ma on hornblende and biotite, respectively, for a granodiorite gneiss from the Rio Jicaya region (fig. 3).

Analytical Techniques

Rock and mineral separations were carried out at the Westfälische Wilhelms-Universität in Münster (Zentrallabor für Geochronologie). Pegmatite samples were carefully crushed by hammer, and different micas and feldspars were separated using a fine needle and tweezers. To isolate the crystal

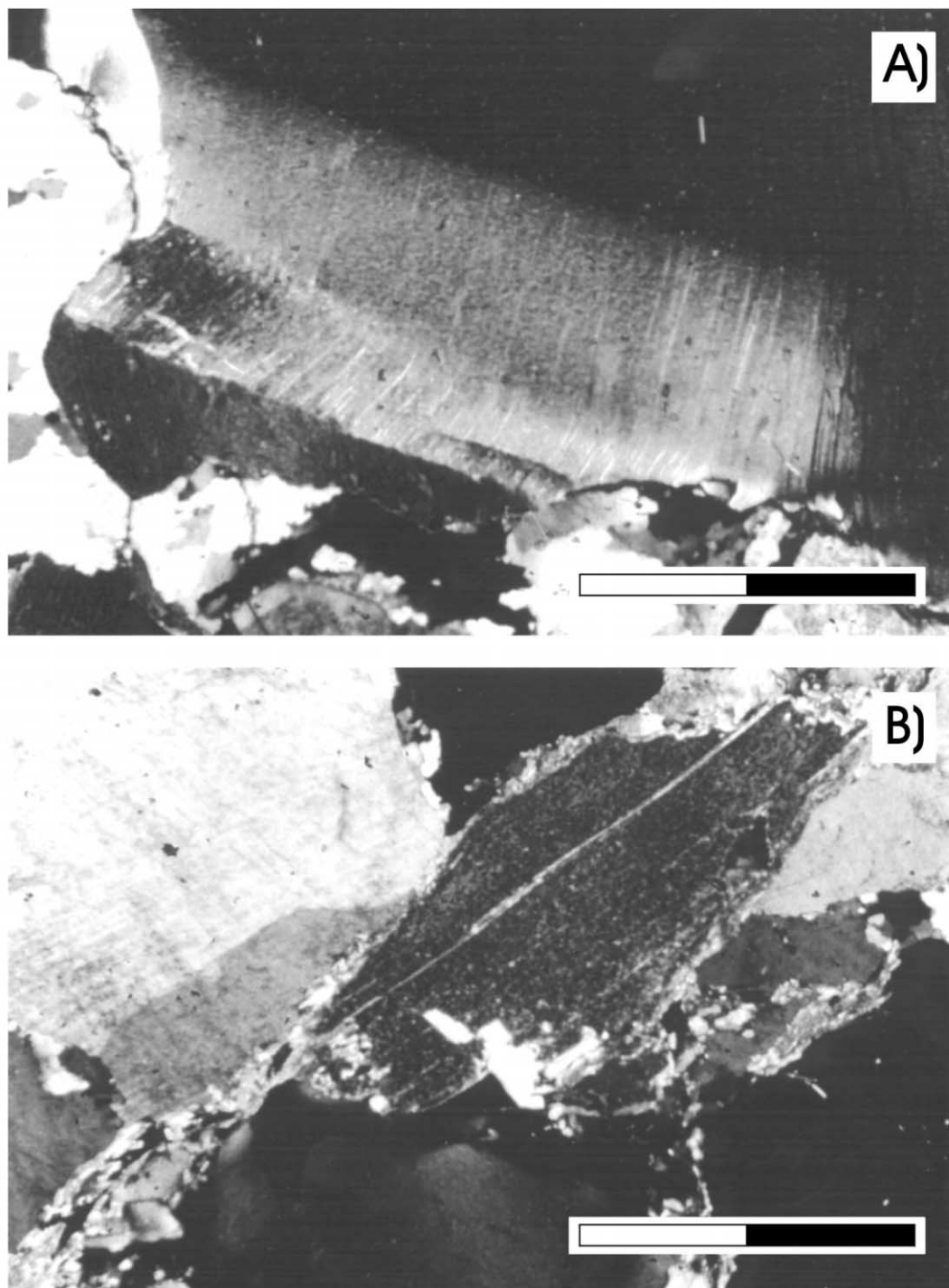


Figure 4. Microphotographs of white mica in the pegmatite S141[RJ]. *A*, Kinked rim of a coarse-grained white mica (generation 1) with typically undulatory extinction; *B*, orientated medium-grained white mica (generation 1) mantled by fine-grained white mica (generation 2), crossed-polarized light; scale represents 1 mm.

cores, the outer rims of coarse-grained white mica in pegmatites were simply cut away with scissors. Bulk separates of white mica were analyzed for sample S157[MJ]. Mineral separates (355–500 μm) of the granodiorite and biotite gneiss were also prepared as bulk separates obtained by crushing, sieving, and magnetic separation. All mineral separates were purified by hand-picking and ultrasonically cleaned in order to remove surface contaminants. Whole-rock powders were obtained by crushing cleaned pegmatite material (3–4 kg).

X-ray fluorescence (XRF) analyses were performed at the Ruhr-Universität Bochum with a Philips PW 1400 XRF spectrometer (WDX). FeO, H₂O, and CO₂ were determined following the methods of Ungethüm (1965), Fischer (1935), and Hermann and Knake (1973), respectively.

Inductively coupled plasma-mass spectrometry (ICP-MS) analyses of trace elements were commercially performed on an Elan 6000 ICP-MS at Acme Analytical Laboratories in Canada. Eu determination for samples having Ba contents $>\sim 9000$ ppm is problematic; therefore such Eu data have to be considered as semiquantitative.

Mineral analyses were also performed at the Ruhr-Universität-Bochum with a Cameca SX50 electron microprobe. Operating conditions were a 15-kV accelerating voltage, 10-nA beam current, and an integration time of 20 s. Pure oxides, as well as natural and synthetic silicates, were used as standards. Corrections for atomic number, fluorescence, and absorption were carried out using the PAP procedure (parabolic correction after Pichou and Pichoir 1984) supplied by Cameca. The amount of ferric iron in garnet was determined by charge balance after normalization to fixed oxygen and cation numbers. The program Mincalc (H.-J. Bernhard, pers. comm.) was used for the calculation of the structural formulae.

Laser $^{40}\text{Ar}/^{39}\text{Ar}$ analyses were performed at the CLAIR geochronologic facility at the Massachusetts Institute of Technology. Before isotopic analysis, single crystals of muscovite were prepared and irradiated as described by Hodges et al. (1994). The J -value for all of these samples is within 0.00318 ± 0.00002 ($\pm 2\sigma$). Individual analyses were obtained by fusion of single crystals with an argon-ion laser and subsequent analysis with a MAP 215-50 mass spectrometer. Radiogenic yields for the analyses typically exceed 95%, and the precision of age determinations ranges between 1% and 2%. Evaluation of the data with standard isotope correlation diagrams indicates the analyses are dominated by in situ radiogenic argon with minor ad-

dition of modern, atmospheric argon. The ages represent weighted means.

Rb-Sr isotope analyses were performed at the Westfälische Wilhelms-Universität in Münster (Zentrallabor für Geochronologie). For the Rb-Sr analyses, sample quantities between 1 and 100 mg of whole-rock powder, white mica, feldspar, and biotite were spiked with a suitable $^{87}\text{Rb}/^{84}\text{Sr}$ mixed spike and subsequently digested in Savillex-PTFE vials with a mixture of HF/HNO₃ (5 : 1) at 120°C. Complete dissolution was achieved within 2–3 d. After evaporation, the samples were digested a second time in 6 N HCl. Separation of Rb and Sr was performed in 2.5 N HCl using quartz glass columns with Dowex AG-50 W*8 (200–400-mesh ion exchange resin).

Rb was measured on a Teledyne SS 1290, whereas Sr was measured on a VG SECTOR 54. On the basis of repeated analyses of NBS Rb-standard SRM 607, a mass discrimination factor of 0.9939 was used. Exponential mass fractionation correction (Russell et al. 1978; Wasserburg et al. 1981) was applied to Sr. Because of a negligible deviation of 0.006% of the mean value of repeated Sr-standard measurements from the certified value of National Bureau of Standards Sr-standard SRM 987, no further correction of isotope data was necessary. Total blanks were <0.05 ng for Rb and <0.1 ng for Sr. An $^{87}\text{Sr}/^{86}\text{Sr}$ ratio of 0.71, as determined in a mixture of the used reagents, was employed for the calculations. A minimum uncertainty of 1% (2σ) on the $^{87}\text{Rb}/^{86}\text{Sr}$ ratio was estimated from replicate analyses and therefore applied for all isochron calculations. Isochron calculations were carried out according to York (1969). All errors on ages are given as 2σ .

Bulk-Rock Geochemistry

Major- and trace-element analyses of 12 granitoid rocks and one metamorphic sample of the country rock are summarized in table 1 (tables 1–4 are available from *The Journal of Geology* free of charge upon request). The biotite gneiss country rock F019[RJ] in Jicaya valley shows slightly higher FeO + Fe₂O₃, CaO, MgO, and TiO₂ than the granitoid intrusions (table 1). K₂O is comparable, whereas Na₂O is distinctly lower.

As indicated by their mineralogy and chemistry, the younger pegmatites have a granitic composition (SiO₂ > 70 wt %). The granodiorites also exhibit very SiO₂-rich compositions (>70 wt %). The alkali elements Na and K are strongly enriched, with low K/Na in the samples from Rio Jicaya, intermediate K/Na in the pegmatites of Manicaragua-Jibacoa, and high K/Na in the Yayabo pegmatites. This relation-

ship is also reflected in the Rb/Sr, Rb/Ba, and Rb/K ratios. Generally, it was established that the granitoids are rich in most large ion lithophile elements (LILE). Very high contents of Ba were found in pegmatite S141[RJ] from Rio Jicaya. A systematic survey of the mineral chemistry of the rock-forming minerals (tables 2–4) revealed a maximum celsian component of 16.5 mol % in K-feldspar, as well as Ba-enriched rims of white mica having up to 19 mol % of the theoretical Ba end-member ("oellacherite").

The observed pattern of Ba distribution within the crystals can be interpreted as a primary Ba enrichment, presumably inherited from the source region and followed by subsequent remobilization (M. Krebs, C. Grevel, F. Grafe, W. V. Maresch, K. Stanek, G. and Millán, unpub. data). The high field strength elements (HFSE) are slightly enriched compared with the primitive mantle values reported by Hofmann (1988), having absolute abundances very similar to normal midocean ridge basalts (N-MORB). The observed subchondritic Nb/Ta ratios (mean ~6) are unusual for high-potassium island-arc rocks. Superchondritic Nb/Ta values (up to 33) were reported from potassic arc rocks by Stolz et al. (1996), as well as by Jochum and Hofmann (1998).

On the basis of low initial $^{87}\text{Sr}/^{86}\text{Sr}$ values (<0.7050) obtained from mineral isochrons, we suggest that the Sr is most likely derived from the mantle, without participation of large amounts of old upper crustal lithosphere (Grafe et al. 1997). A systematic analysis of isotope geochemistry in the granitoids and a comparison with the Cretaceous island-arc rocks of Cuba will be presented elsewhere (K. P. Stanek, F. Grafe, A. Renno, and A. Risse, unpub. data).

Geochronology

Presentation of Data. Rocks and minerals were analyzed for their Rb-Sr and $^{40}\text{Ar}/^{39}\text{Ar}$ systematics. Isotope data and age information are summarized in tables 5–7. Fractions of coarse-grained white mica (CWM) and fine-grained white mica (FWM) were treated separately, assuming that the obtained ages reflect different stages of rock development.

Isochron diagrams are depicted in figure 5. High to very high $^{87}\text{Rb}/^{86}\text{Sr}$ ratios (e.g., 12,600; CWM2 in pegmatite G2057[Y]) are typical for the cores of coarse-grained white mica. Several isochrons were calculated for samples S141[RJ], G2057[Y], and G2061[Y] (isochrons 1, 2, and 3 in fig. 5), where the oldest age for each rock is represented by isochron 1. Isochron 2 indicates a subsequent event, and isochron 3 represents isotopic closure of the Rb-Sr sys-

tem in biotite. CWM3 of sample G2061[Y] was not used in the calculation of isochron 1 or in the calculation of isochron 2 because the isotopic data of the whole rock and CWM3 would have yielded an intermediate date (cf. CWM3 in tables 5, 6). This is interpreted to be the result of mixing of primary ("crystallization") and secondary ("metamorphic") mica isotopic components. Thus, CWM3 is probably composed of a primary core and a larger portion of deformed rim (fig. 4A). CWM2 resembles CWM3; however, it has the best intact primary Rb-Sr system preserved in its core and was best separated from the modified rim. In contrast, CWM1 was completely reset during modification with regard to its Rb-Sr systematics. Resetting of the Rb-Sr system must also be assumed for coarse-grained white mica of pegmatite S141[RJ], where CWM2 plots on isochron 2 ("metamorphic").

The relatively high $^{87}\text{Rb}/^{86}\text{Sr}$ ratios in samples G2057[Y] and G2061[Y] suggest that coarse-grained feldspar, as well as fine-grained feldspar from shear zones within the pegmatites, is a mixture of plagioclase and potassium feldspar. The separation technique used precludes complete achievement of pure coarse-grained plagioclase and potassium feldspar samples. Furthermore, local kaolinization of the coarse-grained feldspar was observed. As a consequence, the Rb-Sr systematics of feldspar from all three pegmatites are slightly disturbed. For this reason, they were not used for the isochron calculations. Whole-rock analyses were taken instead. This is possible because of the high $^{87}\text{Rb}/^{86}\text{Sr}$ ratios of white mica and consequently the small influence of data points with a low $^{87}\text{Rb}/^{86}\text{Sr}$ ratio on the calculated age. In this case the error on linear regression is predominantly determined by the uncertainty on the $^{87}\text{Sr}/^{86}\text{Sr}$ measurement of data points with high $^{87}\text{Rb}/^{86}\text{Sr}$ ratios. For the isochron calculations of samples F009[Y], F012[Y], and F019[Y], all data points were used. The age of S157[MJ] (tables 5, 6, 8) was obtained by isochron calculation using isotope data of undifferentiated white mica and feldspar, as well as a representative whole-rock sample. Therefore, a mixing of primary and secondary age information is likely, but the relatively large 2σ error of about 4 Ma does not allow any further interpretation.

Laser $^{40}\text{Ar}/^{39}\text{Ar}$ ages were determined by fusion of single crystals. For this reason, fine-grained white mica and undifferentiated white mica were selected from pegmatite S141[Y] and granodiorite F012[Y], respectively. Ar-isotope data and calculated ages are presented in table 7.

Interpretation of the Calculated Ages. Ages of primary, coarse-grained white mica (isochron 1 of

Table 5. Rb-Sr Isotopic Composition

Sample/analysis	Grain size (mm)	Rb (ppm)	Sr (ppm)	$^{87}\text{Rb}/^{86}\text{Sr}$	$^{87}\text{Sr}/^{86}\text{Sr}$	$\pm 2\sigma$
Pegmatite (S141[RJ]):						
WR	...	23.379	644.48	.1049	.703467	25
CWM3	3–8	434.26	37.773	33.384	.744979	39
CWM4	3–8	384.84	42.605	26.206	.736020	33
CWM1	3–8	355.44	50.009	20.616	.728901	44
FWM	<1	128.46	68.595	5.4195	.709846	46
CWM2	3–8	135.09	69.543	5.6216	.710153	26
BT	<1	269.65	36.942	21.155	.725224	38
CFS1	3–8	89.112	588.27	.4381	.703791	32
CFS2	3–8	19.220	848.44	.0655	.703348	49
CFS3	3–8	8.9971	2010.7	.0129	.703338	22
Pegmatoid (F009[RJ]):						
WR	...	4.9138	472.77	.0301	.703456	18
CWM1	10–15	144.20	39.916	10.461	.716243	43
CWM2	10–15	184.30	26.395	20.242	.727805	79
CWM3	10–15	145.39	58.337	7.2140	.712280	28
CWM4	10–15	186.04	23.445	23.012	.731670	68
CFS1	10–15	.6650	623.70	.0031	.703434	25
Granodiorite (F012[RJ]):						
WR	...	10.225	433.71	.0682	.703433	22
WM1	1–2	124.56	47.344	7.6151	.712199	25
WM2	1–2	124.62	55.879	6.4543	.710911	29
PLAG	<1	(~1) ^a	(~480) ^a	.0069	.703354	25
Biotitegneiss (F019[RJ]):						
WR	...	10.627	251.91	.1220	.703131	25
BT	<1	176.20	17.098	29.893	.733934	41
PLAG	<1	.3395	208.62	.0047	.702947	21
Pegmatite (G2057[Y]):						
WR	...	101.16	28.289	10.354	.715444	32
CWM1	10–20	629.09	.6613	3984.6	5.28554	61
CWM3	10–20	661.39	.4001	10,500	12.9387	90
CWM2	10–20	460.35	.2573	12,591	15.348	15
FWM	<1	261.10	3.1438	246.30	.96295	10
CFS1	10–20	38.461	61.238	1.8168	.706051	24
CFS2	10–20	99.102	66.603	4.3054	.708659	23
FFS	<1	22.899	43.724	1.5151	.706689	12
Pegmatite (G2061[Y]):						
WR	...	196.38	38.138	14.916	.720879	29
CWM2	5–15	518.50	1.2619	1369.8	2.26475	20
FWM3	<1	470.06	4.1852	336.06	1.057157	42
FWM1	<1	473.88	3.4323	416.62	1.1470	13
FWM2	<1	489.59	2.9594	503.76	1.243815	94
CWM1	5–15	496.40	2.3899	640.70	1.3839	11
CWM3	5–15	501.52	2.1410	730.77	1.507687	32
CFS1	5–15	286.77	42.231	19.681	.725857	25
CFS2	5–15	318.29	53.288	17.307	.722790	24
FFS	<1	106.84	30.991	9.9821	.71563	17
Pegmatite (S157[MJ]):						
WR	...	62.014	124.15	1.4448	.705188	22
FS	...	38.928	95.686	1.1767	.704951	23
WM	...	276.13	43.648	18.335	.725394	23

Note. WR = whole rock; CWM = coarse-grained white mica; CFS = coarse-grained feldspar; FWM = fine-grained white mica; FFS = fine-grained feldspar; PLAG = plagioclase; BT = biotite; FS = feldspar/not specified; WM = white mica/not specified.

^a Estimated concentration.

S141[Y], G2057[Y], and G2061[Y]), especially of their non-reequilibrated core portions, represent cooling ages but are interpreted as minimum ages of pegmatite crystallization. The coarse-grained white mica of the pegmatitic apophysis F009[RJ] in granodiorite F012[RJ] yields an age that agrees well

with the age defined by isochron 1 of pegmatite S141[Y]. Thus, this age is also assumed to represent the time of crystallization.

The intermediate age data of coarse-grained white mica CWM3 in G2061[Y] and S157[MJ] (table 8) must be interpreted as the result of mixing of

Table 6. Rb-Sr Isochron Age Data

Sample/isochron	Calculated ages (Ma)	Initial $^{87}\text{Sr}/^{86}\text{Sr}$
Pegmatite (S141[RJ]):		
WR-CWM1-CWM4-CWM3	$87.6 \pm .4$	$.70334 \pm 3$
WR-FWM-CWM2	$84.9 \pm .9$	$.70334 \pm 3$
WR-BT	73 ± 1	$.70336 \pm 2$
Pegmatoid (F009[RJ]):		
CFS-WR-CWM1-CWM2-CWM3-CWM4	$86.2 \pm .5$	$.70342 \pm 3$
Granodiorite (F012[RJ]):		
PLAG-WR-WM2-WM1	$82.1 \pm .6$	$.70335 \pm 2$
Biotite gneiss (F019[RJ]):		
PLAG-WR-BT	73 ± 3	$.70297 \pm 6$
Pegmatite (G2057[Y]):		
WR-CWM1-CWM3-PMW2	$81.8 \pm .4$	$.7034 \pm 2$
WR-FWM	74 ± 1	$.7046 \pm 2$
WR-CWM2	80 ± 1	$.7039 \pm 2$
WR-FWM1-FWM2-FWM3-CWM1	$74.6 \pm .7$	$.7051 \pm 3$
WR-CWM3	77 ± 1	
Pegmatite (S157[MJ]):		
FS-WR-WM	84 ± 4	$.70350 \pm 5$

Note. WR = whole rock; CWM = coarse-grained white mica; CFS = coarse-grained feldspar; FWM = fine-grained white mica; FFS = fine-grained feldspar; PLAG = plagioclase; BT = biotite; FS = feldspar/not specified; WM = white mica/not specified.

two sources of different age information preserved in an isotopically polyphase crystal. These dates therefore do not have any real geological meaning.

The ages of fine-grained white mica and isotopically reset coarse-grained white mica (isochron 2 of S141[Y], G2057[Y], and G2061[Y]) are interpreted to represent maximum ages for shear-zone formation in pegmatites because at least partial isotopic reequilibration between white mica and feldspar can be assumed in these samples. The age of the white mica in granodiorite F012[RJ] is significantly younger than the “crystallization” ages of pegmatites S141[RJ] and F009[RJ]. This age is even younger than the “metamorphic” age (isochron 2) of S141[RJ]. Keeping in mind that the metamorphic age of S141[RJ] represents only a maximum age of reequilibration, the white mica age of F012[RJ] may reflect a lower age limit to metamorphism (possibly the cessation of this overprinting episode).

Laser $^{40}\text{Ar}/^{39}\text{Ar}$ ages of 72.2 ± 0.6 Ma (G2061[Y]) and 73.8 ± 0.5 Ma (F012[Y]) were calculated from Ar-isotope analyses (table 7). These ages are considerably younger than the corresponding Rb-Sr ages for the coarse muscovite phenocrysts discussed above. Within analytical uncertainty, these values are the same as the Rb-Sr ages determined for biotite from sample F019[J] and sample S141[J] (fig. 5). Therefore, the $^{40}\text{Ar}/^{39}\text{Ar}$ muscovite ages ($T_c = 350^\circ\text{--}400^\circ\text{C}$; Mezger 1990) and Rb-Sr biotite ages ($T_c = \sim 350^\circ\text{C}$; Mezger 1990) of ca. 73 Ma are interpreted to reflect cooling through closure temperatures in the range of $350^\circ \pm 50^\circ\text{C}$, subsequent to either crystallization at presumably $600^\circ\text{--}700^\circ\text{C}$

or epidote-amphibolite-facies metamorphism of country rock at $620^\circ\text{--}640^\circ\text{C}$. The identical laser $^{40}\text{Ar}/^{39}\text{Ar}$ ages on muscovite and Rb-Sr ages on biotite in pegmatite, granodiorite, and country rock show that the “cooling” age is representative of the whole metamorphic complex of Rio Jicaya valley.

Crystallization and metamorphic ages could also be determined for the pegmatite samples from Yayabo quarry. However, crystallization ages are younger by $\sim 4\text{--}7$ Ma and metamorphic ages by $8\text{--}11$ Ma than those of Rio Jicaya. All ages and their geological interpretations are summarized in table 8.

Discussion of Results

Geochronology of Granitoid Intrusives. The Rb-Sr systematics of primary coarse-grained white mica provides essential information on the time of crystallization of the pegmatites and places a minimum age limit on the time of epidote-amphibolite-facies metamorphism for the Mabujina formation. Intrusion of pegmatites occurred at ~ 88 Ma in the Rio Jicaya region and at ~ 81 Ma in the Yayabo region.

The K-Ar date of $\sim 85 \pm 4$ Ma (Somin and Millan 1981) on white mica from a pegmatoid vein northwest of the Yayabo quarry agrees within error with the crystallization age of the Yayabo pegmatite. However, this K-Ar age is not comparable to the Rb-Sr crystallization age from the Yayabo quarry because the relative age position of this pegmatoid vein (within the Yayabo unit) to the granitic pegmatite (within the Mabujina unit) is not clear. If both rocks had the same relative age position, the

Table 7. Ar-Isotope Data

Analysis	$^{40}\text{Ar}^*$	^{39}Ar (K)	^{38}Ar (Cl)	^{37}Ar (Ca)	^{36}Ar (atm)	K/Ca	K/Cl	Ca/Cl	$^{40}\text{Ar}^*$ (%)	Age (Ma)
Fine-grained white mica of pegmatite 2061—Yayabo Quarry										
11	5.640 ± 53	$.4423 \pm 18$	$.000313 \pm 04$	$.000031 \pm 40$	$.000944 \pm 83$	7385.8	150.1	.020	95.3	71.8 ± 1.2
12	4.861 ± 42	$.3738 \pm 13$	$.000383 \pm 06$	$.000099 \pm 60$	$.000736 \pm 79$	1970.2	103.9	.053	95.7	73.2 ± 1.4
13	5.909 ± 52	$.4629 \pm 33$	$.000774 \pm 12$	$.000278 \pm 70$	$.001269 \pm 84$	866.9	63.6	.073	94.0	71.9 ± 1.3
14	5.079 ± 61	$.3935 \pm 32$	$.000302 \pm 05$	$.000130 \pm 60$	$.001131 \pm 77$	1579.4	138.7	.088	93.8	72.6 ± 1.5
15	8.090 ± 39	$.6370 \pm 13$	$.000464 \pm 06$	$.000484 \pm 70$	$.001673 \pm 81$	684.6	146.0	.213	94.2	$71.5 \pm .8$
Average										$72.2 \pm .6$
White mica of granodiorite F012—Rio Jicaya										
6	5.702 ± 41	$.4357 \pm 12$	$.000647 \pm 8$	$.000445 \pm 090$	$.000420 \pm 40$	509.1	71.6	.141	97.9	$74.7 \pm .8$
7	5.940 ± 41	$.4604 \pm 13$	$.000646 \pm 5$	$.000608 \pm 050$	$.000868 \pm 52$	393.5	75.8	.193	95.9	$73.7 \pm .8$
8	8.255 ± 43	$.6441 \pm 08$	$.000745 \pm 7$	$.000859 \pm 100$	$.001184 \pm 52$	389.9	92.0	.236	95.9	$73.2 \pm .6$
9	6.886 ± 43	$.5342 \pm 14$	$.000862 \pm 7$	$.000806 \pm 070$	$.001045 \pm 36$	344.4	65.9	.191	95.7	$73.6 \pm .7$
10	5.356 ± 39	$.4149 \pm 26$	$.000460 \pm 5$	$.000447 \pm 060$	$.000519 \pm 37$	482.9	95.9	.199	97.2	73.7 ± 1.0
Average										$73.8 \pm .5$

Note. Average = average age representing the weighted mean having a 2σ standard error; atm = atmospheric; asterisks indicate radiogenic argon.

K-Ar date should be significantly younger because the closure temperature of the K-Ar system in white mica is $\sim 350^\circ\text{--}400^\circ\text{C}$ (Mezger 1990). An explanation for a possible overestimation of an age obtained by the conventional K-Ar method could be the participation of excess ^{40}Ar in the sample because no "magmatic" or "metamorphic" excess ^{40}Ar was considered in the age calculation (Faure 1986). A generally high amount of excess ^{40}Ar in pegmatitic rocks was observed by Laughlin (1969). Therefore we strongly recommend that this age and even other similar K-Ar ages from Mabujina amphibolite be redetermined using $^{40}\text{Ar}/^{39}\text{Ar}$ methods to avoid the effects of excess ^{40}Ar .

The contrasting Rb-Sr isotope data of white mica in shear zones and fine-grained white mica of weakly overprinted granodiorite intrusions are interpreted to indicate isotopic reequilibration at temperatures lower than $450^\circ\text{--}500^\circ\text{C}$, due to reopening of the isotope system by deformation and/or fluid activity. They may reflect late-metamorphic, postpegmatitic stages of an inhomogeneous, weak, ductile deformation in a still compressive regime. Isotopic reequilibration seems to be grain-size dependent. Age information on crystallization was preserved to different degrees in the core portions of large coarse-grained white mica in pegmatites, but fine-grained white mica of granodiorite have totally lost their primary age information.

Cooling ages obtained from Rb-Sr analyses on biotite of the pegmatitic intrusion S141[RJ] and biotite of surrounding, metamorphosed country rock F019[RJ], as well as from laser $^{40}\text{Ar}/^{39}\text{Ar}$ analyses on white mica of the pegmatitic G2061[Y] and granodioritic intrusion F012[RJ] partly outline the cooling history of the Mabujina unit.

Thermochronological data of granitoid intrusives and Mabujina rocks result in a T - t path for these rocks as shown in figure 6. The granitoid intrusions cooled rapidly following intrusion into the epidote-amphibolite-facies Mabujina formation. With time, the cooling rate decreased until it became the same as the cooling rate of the surrounding Mabujina unit. The small arrows indicate that the T_c for the Rb-Sr system in the metamorphic white mica can be affected by deformation and/or fluid activity, and therefore should rather be somewhat below those of the coarse-grained white mica.

Regional Implications. On the basis of field and structural data, we interpret the eastern part of the Escambray Massif to represent a tectonic nappe pile, of which the uppermost part consists of the Mabujina unit. The underlying tectonic units partly contain HP metamorphic rocks of still enigmatic age.

The dating of the late- to postmetamorphic intrusions into the folded epidote-amphibolite-facies rocks of the Mabujina formation and their cooling history are thus also critical for the T - t evolution of the Escambray rocks. Thus, HP metamorphism must have taken place and ceased before the regional exhumation of the Mabujina unit started, that is, before late Campanian time (ca. 70 Ma). Therefore, metamorphism and ductile deformation of the Escambray rocks were completed at least 10 m.yr. before the inactive island arc was thrust onto the southern margin of the Bahamas Platform starting around 60 Ma (Pardo 1975).

Recent paleotectonic models of the northern Caribbean (e.g., Pindell 1993, 1994; Stanek and Voigt 1994; Stanek 2000) suggest that an island-arc system was moving northward and northeastward dur-

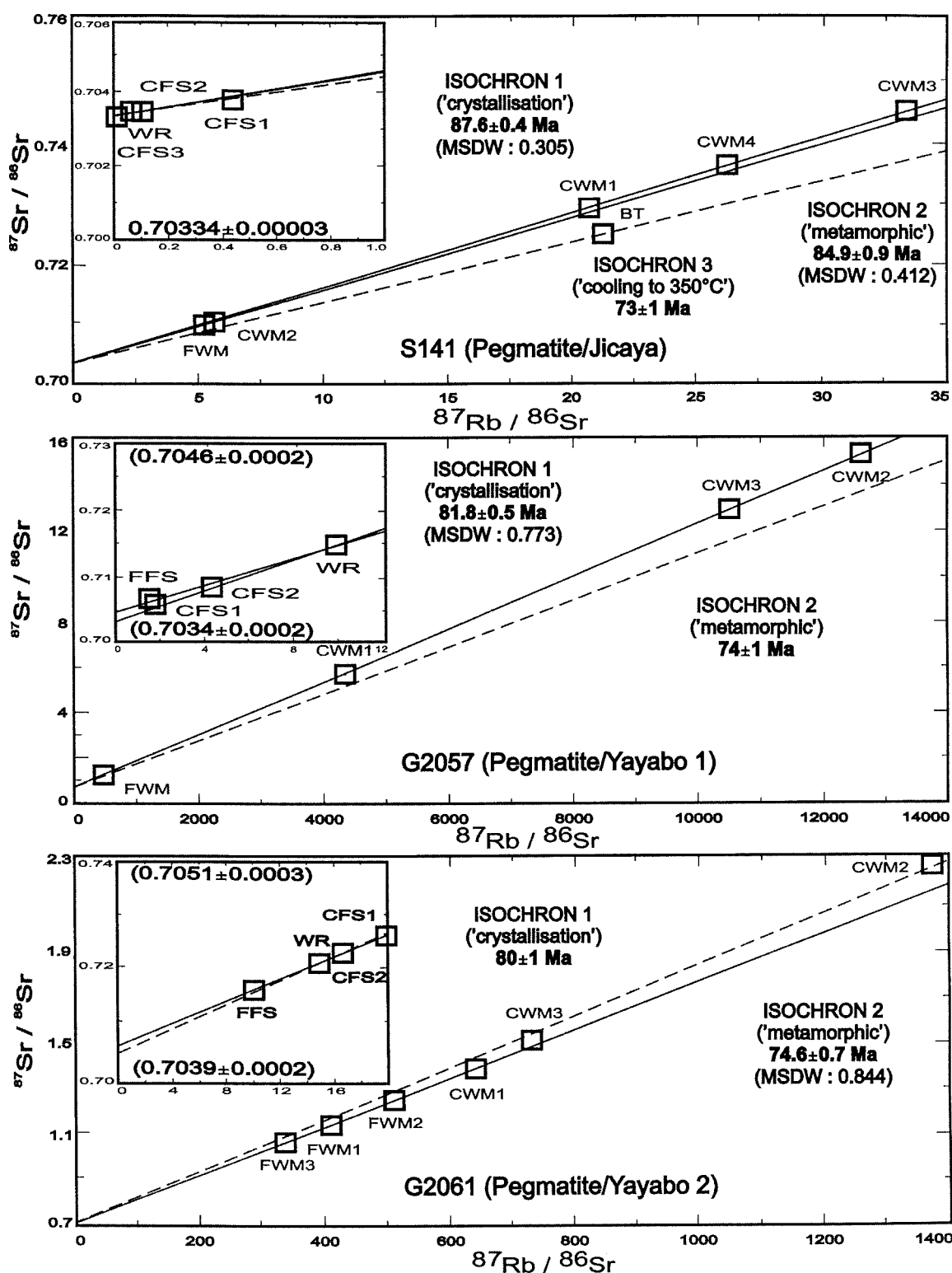


Figure 5. Rb-Sr isochron diagrams for selected samples. WR = whole rock; CWM = coarse-grained white-mica; FWM = fine-grained white-mica; CFS = coarse-grained feldspar; FFS = fine-grained feldspar; PLAG = plagioclase; BT = biotite; FS = feldspar/not specified; WM = white mica/not specified; MSWD = mean square of weighted deviates, after McIntyre et al. 1966.

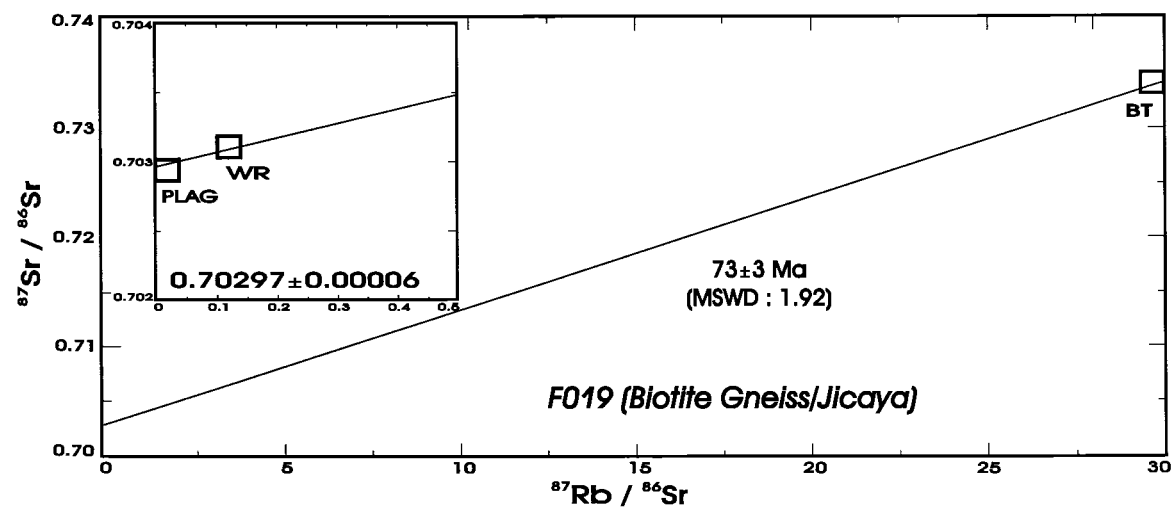
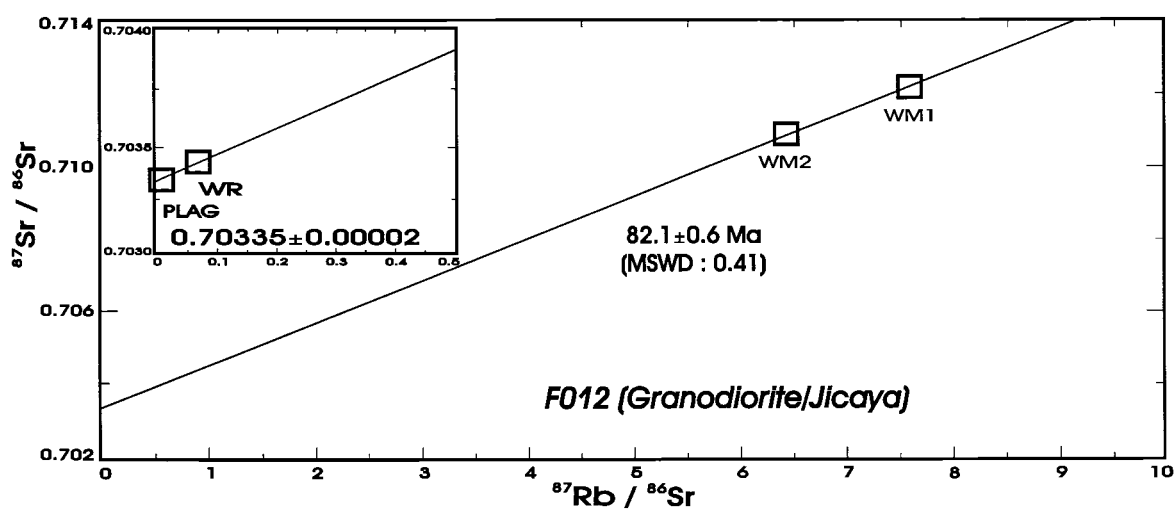
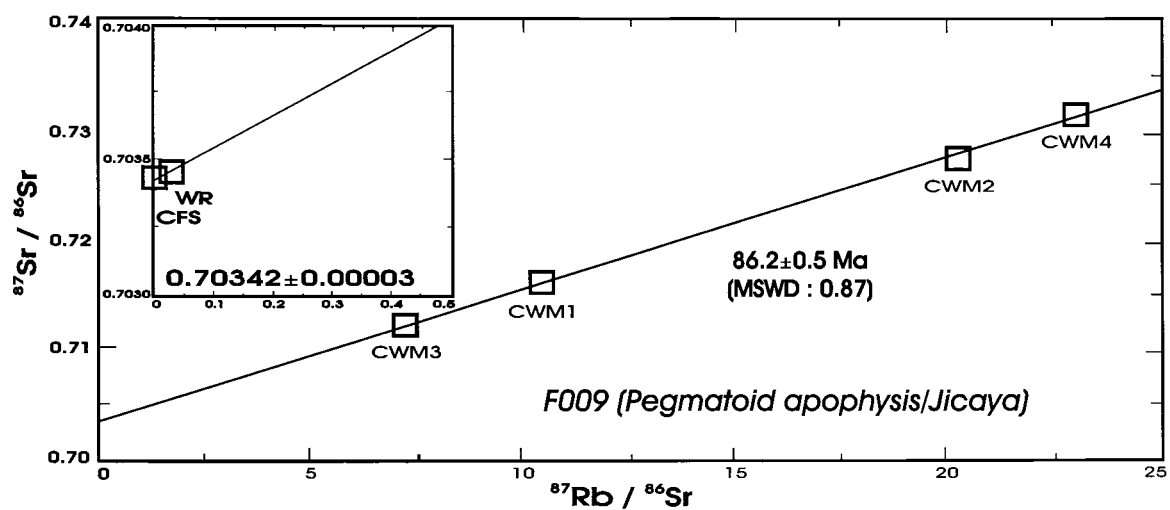


Figure 5 (Continued)

Table 8. Rb-Sr and $^{40}\text{Ar}/^{39}\text{Ar}$ Ar Data

Definition	Rio Jicaya				Road M.- Jibacoa	Yayabo Quarry	
	Pegmatite		Granodiorite	Biotite gneiss	Pegmatite	Pegmatite	
	S141	F009	F012	F019	S157	G2057	G2061
"Crystallization" Age ^a	87.6 ± .4	86.2 ± .5	81.8 ± .4	80 ± 1 77 ± 1
"Mixing" Age ^b	84 ± 4	...	(CWM3)
"Metamorphic" Age ^c	84.9 ± .9	...	82.1 ± .6	74 ± 1	74.6 ± .7
Cooling Age ^d	73.8 ± .5	72.2 ± 0.6
Cooling Age ^e	73 ± 1	73 ± 3
Initial $^{87}\text{Sr}/^{86}\text{Sr}$ value	.70334 ± .0003	.70342 ± .00003	.70335 ± .00002	.70297 ± .00006	.70351 ± .00011	~.7040	~.7050

Note. Ages in Ma.

^a Rb-Sr age on primary coarse-grained white mica; $T_c = 450^\circ\text{--}500^\circ\text{C}$.

^b Mixing of primary and secondary Rb-Sr age information.

^c Rb-Sr age on fine-grained white mica from shear zones.

^d $^{40}\text{Ar}/^{39}\text{Ar}$ age on fine-grained white mica; $T_c = 350^\circ\text{--}400^\circ\text{C}$.

^e Rb-Sr age on fine-grained biotite; $T_c = 350^\circ\text{C}$.

ing the mid-Cretaceous due to the motion of the Pacific (Farallon) plate. The island arc initially collided with the southern edge of the sedimentary platform of the Yucatán Peninsula in the Late Cretaceous (Stanek and Voigt 1994; Stanek 2000; Stanek et al. 2000). However, little is known about the early history of the collision in this region because of the tectonic overprinting by younger strike-slip motions along the Motagua fault zone. At this time the sedimentation east of the Yucatán Peninsula and south of the Bahamas Platform was interrupted, and an influence on the sedimentation regime caused by the island arc can be observed. This seems to correlate with the end of epidote-amphibolite-facies metamorphism of the Mabujina rocks and the intrusion of post- to late-metamorphic granitoid rocks. Following the existing thermochronological data, the juxtaposition of the Mabujina unit and the Yayabo unit, as well as the initial cooling of the Mabujina unit, ended at ~90 Ma (fig. 6). The collision of the north-facing arc with the southern edge of the Yucatán Peninsula probably caused a change in subduction conditions involving thermal relaxation without notable uplift.

We infer that during such an episode, the Mabujina rocks were cooled from lower amphibolite to greenschist facies conditions. Granitic magma from lower parts of the island arc intruded the Mabujina metamorphic rock assemblage without being affected by conditions of epidote-amphibolite-facies metamorphism.

After this last magmatic episode, the whole island arc cooled further and the upper parts of the island arc were eroded. Extensive mid-Campanian (ca. 80 Ma) to upper Maastrichtian (70–65 Ma) car-

bonate sequences (including peneplanation and transgression) indicate that the Late Cretaceous was a period of relative tectonic stability.

Uplift to higher crustal levels and exhumation of Mabujina rocks is evident from the geological record of post-Cretaceous sedimentary basins in the periphery of the recent Escambray Massif (fig. 2). I. Kanchev (unpub. data, 1978) reported the occurrence of latest upper Cretaceous carbonate blocks of several tens of meters in a fanglomeratic carbonate matrix at the Paleocene-Eocene boundary (60 Ma), and since the upper Eocene (ca. 45 Ma), the first appearance of terrigenous clastics, including debris of Escambray metamorphic rocks, in the Cienfuegos basin and in the Cabaiguan basin (fig. 1). Debris from Mabujina metamorphic rocks started to occur between 60 and 45 Ma, shortly before Escambray metamorphic rocks arrived at the surface. Additional evidence comes from first fission track dates on zircon from HP metamorphic rocks (M. R. Brix, pers. comm.) of the Escambray Massif underlying the Mabujina rocks. These data indicate cooling to temperatures of $280^\circ \pm 30^\circ\text{C}$ (Stöckhert et al. 1999) and scatter between 68 and 58 Ma (Stanek et al. 1998). All these constraints indicate that final cooling, starting at 70–65 Ma, was dominated by uplift, thrusting onto the Bahamas Platform and subsequent exhumation processes.

Conclusions

To summarize and outline the major results, four points are emphasized:

1. The investigated samples of late- to post-

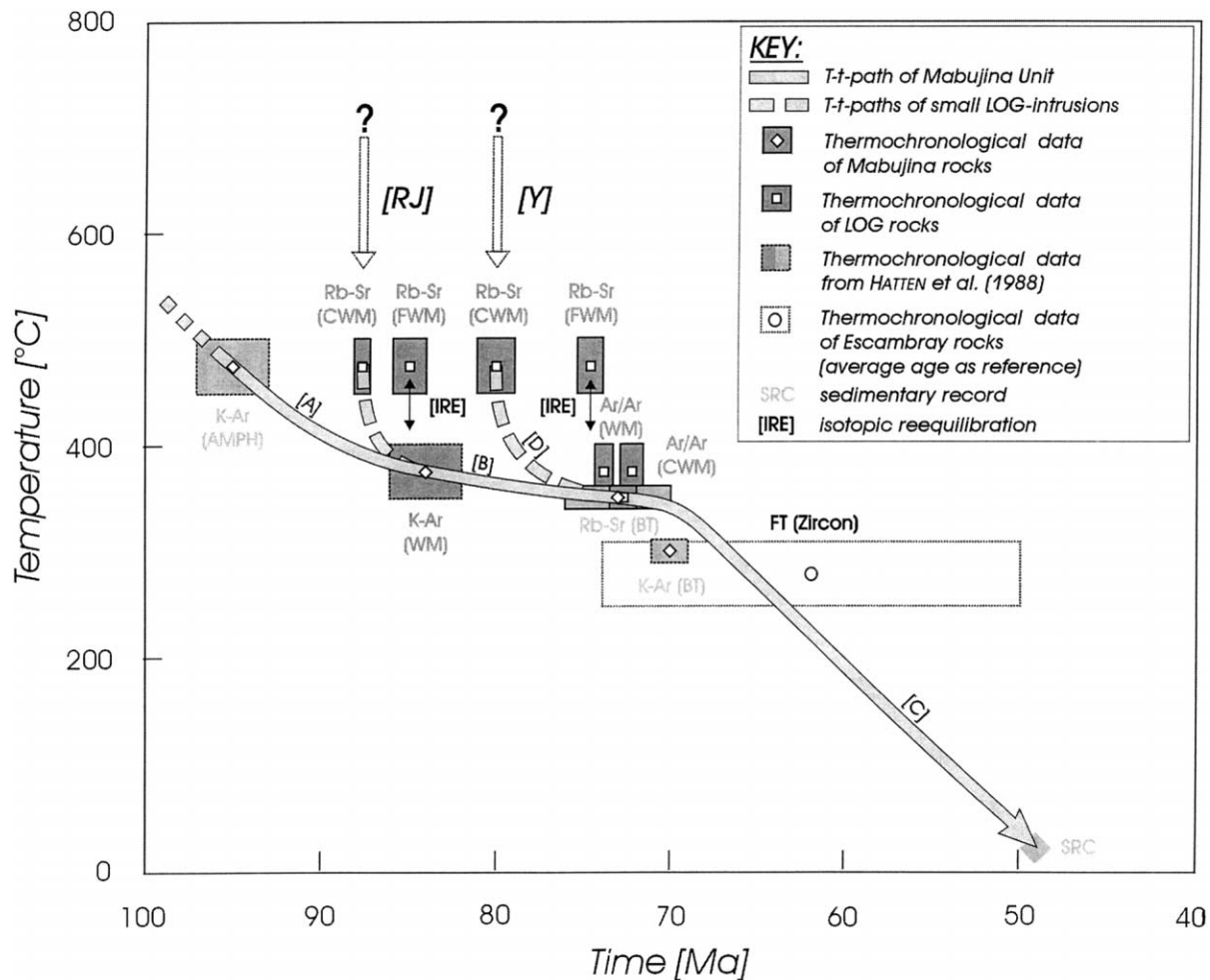


Figure 6. *T-t* path of late-orogenic granitoid intrusions and Mabujina metamorphic rocks. SRC, age estimate by evidence from the sedimentary record of adjacent basins, estimated cooling rates: A, $\sim 9^{\circ}\text{C}/\text{Ma}$; B, $\sim 2^{\circ}\text{C}/\text{Ma}$; C, $\sim 14^{\circ}\text{C}/\text{Ma}$; D, $\sim 13^{\circ}\text{--}38^{\circ}\text{C}/\text{Ma}$.

kinematic intrusives are of granodioritic to granitic composition. Pegmatites are enriched in most LILE. However, they resemble N-MORBs in their HFSE concentrations, and on the basis of their low initial $^{87}\text{Sr}/^{86}\text{Sr}$ values of <0.7050 Sr are very likely to be mantle derived.

2. Rb-Sr crystallization ages of pegmatites place a minimum age limit of 88–80 Ma on (a) the epidote-amphibolite-facies metamorphism in the Mabujina unit, (b) the magmatic activity of the Cretaceous island arc, (c) the onset of the initial collision of the Cretaceous island arc with the southern edge of the Yucatán Peninsula, and (d) the HP metamorphism and juxtaposition of tectonic units of different metamorphic grade in the Escambray Massif.

3. Laser $^{40}\text{Ar}/^{39}\text{Ar}$ ages of muscovite and Rb-Sr

ages of biotite indicate cooling of the Mabujina unit through $350 \pm 50^{\circ}\text{C}$ at ~ 73 Ma.

4. The comparison of the new thermochronological data with evidence for regional uplift and exhumation recorded in adjacent molassoid basins suggests a two-stage collision, where cooling of Mabujina unit rocks was initially driven by a change of the subduction regime combined with thermal relaxation, and subsequently was dominated by regional uplift and exhumation.

ACKNOWLEDGMENTS

We extend our sincere thanks to K. Mezger, Münster, for fruitful discussions on problems of age dating and permission to use the facilities of the Zentrallabor für Geochronologie. H.-J. Bernhardt and

T. Fockenberg, Bochum, provided invaluable assistance with microchemical and whole-rock analyses. We are grateful to M. Brix for fission-track analyses on zircon. This article benefited from a supply of unpublished reports and continuous discussion on the geology of the Mabujina and Escambray by

our Cuban colleagues from the Instituto de Geología y Paleontología in Havana. The study was financially supported by the Deutsche Forschungsgemeinschaft–DFG grants STA362/4-1 and MA 689/13-1.

REFERENCES CITED

- Bibikova, E. B.; Somin, M. L.; Graceva, T. V.; Makarov, V. A.; Millan, G.; and Chukoljukov, J. A. 1988. Perwyje rezultaty U-Pb-datirowanija metamorfitscheskich porod Bolschoi Antilskoi dugi: vosrašt kompleksa mabuchina, Kuby (First results of U-Pb dating on metamorphic rocks from the Greater Antilles Island Arc: the age of the Mabujina complex, Cuba). *Geologija* 301:550–552.
- Brown, E. H. 1977. The crossite content of Ca-amphibole as a guide to pressure of metamorphism. *Petrology* 18: 53–57.
- Faure, G. 1986. *Principles of isotope geology*. New York, Wiley, 589 p.
- Fischer, K. 1935. Neues Verfahren zur meßanalytischen Bestimmung des Wassergehaltes von Flüssigkeiten und festen Körpern (A new method to determine the H₂O-content in fluids and solids). *Angew. Chem.* 48: 394.
- Grafe, F.; Stanek, K. P.; Baumann, A.; Maresch, W. V.; and Millan, G. 1997. Constraints on the age of HT/LP-metamorphism by Rb-Sr dating of pegmatitic rocks, Mabujina unit, Escambray, central Cuba. *Ber. Dtsch. Min. Ges., Beih. Eur. J. Mineral.* 9:136.
- Grevel, C. 2000. Druck- und Temperaturentwicklung der metamorphen Deckeneinheiten des Escambray Massives, Kuba (Pressure and temperature history of the metamorphic nappes of the Escambray Massif, Cuba). Ph.D. thesis, Ruhr-Universität Bochum, Bochum.
- Grevel, C.; Maresch, W. V.; Millan, G.; and Stanek, K. P. 1996. Deerite from the Escambray Massif, Cuba. *Ber. Dtsch. Min. Ges., Beih. Eur. J. Mineral.* 8:79.
- Hatten, C. W.; Somin, M.; Millan, G.; Renne, P.; Kistler, R. W.; and Mattinson, J. M. 1988. Tectonostratigraphic units of central Cuba. In L. Barker, ed. *Transactions of the 11th Caribbean Geological Conference* (Barbados, 1986) vol. 35, p. 1–13.
- Hermann, A. G., and Knake, D. 1973. Coulometrisches Verfahren zur Bestimmung von Gesamt-Karbonat- und Nichtkarbonat-Kohlenstoff in magmatischen und metamorphen Gesteinen (Coulometric method to determine total carbon and non-carbonate carbon in magmatic and metamorphic rocks). *Z. Anal. Chem.* 266:196–201.
- Hodges, K. V.; Hames, W. E.; Olsezewski, W. J.; Burchfiel, B. C.; Royden, L. H.; and Chen, Z. 1994. Thermobarometric and ⁴⁰Ar/³⁹Ar geochronologic constraints on Eohimalayan metamorphism in the Dinggyê area, southern Tibet. *Contrib. Mineral. Petrol.* 117: 151–163.
- Hofmann, A. W. 1988. Chemical differentiation of the Earth: the relationship between mantle, continental crust, and oceanic crust. *Earth Planet. Sci. Lett.* 90: 297–314.
- Hutson, F.; Mann, P.; and Renne, P. 1998. ⁴⁰Ar/³⁹Ar dating of single muscovite grains in Jurassic siliciclastic rocks (San Cayetano Formation): constraints on the paleoposition of western Cuba. *Geology* 26:83–86.
- Iturralde-Vinent, M. A. 1994. Cuban geology: a new plate-tectonic synthesis. *J. Petrol. Geol.* 17:39–70.
- Jochum, K. P., and Hofmann, A. W. 1998. Nb/Ta in MORB and continental crust: implications for a superchondritic Nb/Ta reservoir in the mantle. *EOS: Trans. Am. Geophys. Union* 17:354.
- Laird, J., and Albee, A. L. 1981a. High pressure metamorphism in mafic schist from northern Vermont. *Am. J. Sci.* 281:97–126.
- . 1981b. Pressure-temperature and time indicators in mafic schist: their application to reconstructing the polymetamorphic history of Vermont. *Am. J. Sci.* 281: 127–175.
- Laughlin, A. W. 1969. Excess radiogenic argon in pegmatite minerals. *J. Geophys. Res.* 74:6684–6690.
- Leake, B. E. 1997. Nomenclature of amphiboles: report of the Subcommittee on Amphiboles of the International Mineralogical Association Commission on New Minerals and Mineral Names. *Eur. J. Mineral.* 9: 623–638.
- McIntyre, G. A.; Brooks, C.; Compston, W.; and Turek, A. 1966. A statistical assessment of Rb-Sr isochrons. *J. Geophys. Res.* 71:5459–5468.
- Mezger, K. 1990. Geochronology in granulites. In Vielzeuf, D., and Vidal, P., eds. *Granulites and crustal evolution*. Dordrecht, Kluwer Academic, p. 451–470.
- Millan, G. 1996. Geología del Complejo Mabujina (Geology of the Mabujina Complex). In Iturralde-Vinent, M.A., ed. *Ofolitas y arcos volcanicos de Cuba*. Contrib. 1, Project 364, Miami, IUGS/UNESCO International Geological Correlation Programme, p. 147–153.
- . 1997. Geología del macizo metamórfico Escambray (Geology of the metamorphic Escambray Massif). In G. F. Furrzola Bermudez and K. E. Nunez Cambra, eds. *Estudios sobre la geología de Cuba*. Centro Nacional de Información Geológica, Institut de Geología y Paleontología, Havana, p. 271–288.
- Millan, G., and Myscinski, R. 1978. Fauna Jurasica y con-

- sideraciones sobre la edad de las secuencias metamórficas del Escambray (Jurassic fauna and considerations on the age of the metamorphic sequences of the Escambray). Havana, Informe Científico-Técnico, Academia de Ciencias de Cuba, p. 1–14.
- Millan, G., and Somin, M. L. 1985. Contribution al conocimiento geológico de las metamórficas del Escambray y del Purial (Contributions to the geological knowledge of the metamorphic rocks from the Escambray and Purial). Havana, Academia de Ciencias de Cuba, p. 1–74.
- Pardo, G. 1975. Geology of Cuba. In Nairn, A. E. M., and Stehli, F. G., eds. The ocean basins and margins. Vol. 3. Plenum, New York, p. 553–613.
- Pichou, J. L., and Pichoir, F. 1984. Un nouveau modèle de calcul pour la microanalyse quantitative par spectrométrie de rayons X. *Rech Aérospatiale* 3: 167–192.
- Pindell, J. L. 1993. Determination of Euler pole for relative motion of Caribbean and North American plates using slip vectors of interplate earthquakes. *EOS: Trans. Am. Geophys. Union* 74:586.
- . 1994. Evolution of the Gulf of Mexico and the Caribbean. In Donovan, S. K., and Jackson, T. A., eds. Caribbean geology: an introduction. Kingston, Jamaica, University of the West Indies Pub. Assoc., p. 13–39.
- Russell, W.; Papanastassiou, D. A.; and Tombrello, T. A. 1978. Ca isotope fractionation on the Earth and other solar system materials. *Geochim. Cosmochim. Acta* 42:1075–1090.
- Somin, M. L.; Arakeljan, M. M.; and Kolesnikov, E. M. 1992. Age and tectonic significance of high-pressure metamorphic rocks of Cuba. *Int. Geol. Rev.* 34: 105–118.
- Somin, M. L., and Millan, G. 1974. Nekotoryye cherty struktury mezozoyskikh metamorficheskikh tolshch Kuby (Some structural features of Mesozoic metamorphic sequences in Cuba). *Geotektonika* 5:19–30.
- . 1981. Geologiya metamorfitscheskikh kompleksov Kuby (Geology of metamorphic complexes in Cuba). Moskova, Isdat. Nauka, 219 p.
- Stanek, K. P. 2000. Geotektonische Entwicklung Kubas (Geotectonic evolution of Cuba). *Freiberger Forschungshefte* C476:1–174.
- Stanek, K. P.; Cobiella, J.; Maresch, W. V.; Millan, G.; Grafe, F.; and Grevel, C. 2000. Geological development of Cuba. *Z. Angew. Geol.* SH1:259–265.
- Stanek, K. P.; Grafe, F.; Maresch, W. V.; Baumann, A.; Grevel, C.; and Millan, G. 1998. Nappe tectonics and geochronological implications of metamorphic units in central Cuba. *Freiberger Forschungshefte* C471: 219–220.
- Stanek, K. P., and Voigt, S. 1994. Model of Meso-Cenozoic evolution of the northwestern Caribbean. *Zentral. Geol. Paläontol.* 1–2:499–511.
- Stöckhert, B.; Brix, M. R.; Kleinschrodt, R.; Hurford, A. J.; and Wirth, R. 1999. Thermochronometry and microstructures of quartz: a comparison with experimental flow laws and predictions on the temperature of the brittle-plastic transition. *J. Struct. Geol.* 21: 351–369.
- Stolz, A. J.; Jochum, K. P.; Spettel, B.; and Hofmann, A. W. 1996. Fluid- and melt-related enrichment in the subarc mantle: evidence from Nb/Ta variations in island-arc basalts. *Geology* 24:587–590.
- Sukar, K., and Perez, M. 1997. Granitoides del arco volcánico del la región central de Cuba—antigua provincia de Las Villas (Island arc granitoids of central Cuba—former province of Las Villas). In G. F. Furrzola Bermudez and K. E. Nunez Cambra, eds. Estudios sobre la geología de Cuba. Centro Nacional de Información Geológica, Institut de Geología y Paleontología, Havana, p. 371–386.
- Ungethüm, H. 1965. Eine neue Methode zur Bestimmung von Eisen (II) in Gesteinen und Mineralen, insbesondere auch in bitumenhaltigen Proben (A new method to determine Fe^{2+} in rocks and minerals, applicable in particular to bituminous samples). *Z. Angew. Geol.* 11:500–505.
- Wasserburg, G. J.; Jacobsen, S. B.; DePaolo, D. J.; McCulloch, M. T.; and Wen, T. 1981. Precise determination of Sm/Nd ratios: Sm and Nd isotopic abundances in standard solutions. *Geochim. Cosmochim. Acta* 45:2311–2323.
- York, D. 1969. Least squares fitting of a straight line with correlated errors. *Earth Planet. Sci. Lett.* 5:320–324.